Alexei E. Romanov^a, Glenn E. Beltz^b, James S. Speck^c

^a Ioffe Physico-Technical Institute RAS, Saint Petersburg, Russia

^bUniversity of California, Mechanical Engineering Department, Santa Barbara, USA

^cUniversity of California, Materials Department, Santa Barbara, USA

Crack formation in surface layers with strain gradients

Dedicated to Professor Dr. Wolfgang Pompe on the occasion of his 65th birthday

The problem of crack formation in surface layers where a linear profile of elastic strain prevails through the thickness of a layer is investigated. Such strain gradients can be generated, for example, in graded alloy semiconductor layers or due to specific stress relaxation mechanisms in lattice mismatched layers or previously unanticipated dislocationrelated strain gradients. The operation of the relaxation mechanisms related to threading dislocation inclination and leading to the strain gradients in nominally compressed Al_xGa_{1-x}N layers grown on buffer layers with smaller lattice constants is discussed. A fracture mechanics model is developed for the calculation of the stress intensity factor of mode I cracks initiated at the surface of the layer exhibiting a linear strain dependence. The critical layer thickness for crack formation in such a gradient elastic field has been found in the framework of this fracture mechanics model. Results of the modeling are compared with experimental observations of crack onset in nominally compressed layers of Al_xGa_{1-x}N semiconductors. Good agreement between the model predictions and the experimental data is found.

Keywords: Strain gradient; Crack; III-nitrides; Threading dislocation

1. Introduction

High elastic strains and mechanical stresses in surface layers of engineering and functional materials can be considered as a leading reason for degradation of their mechanical and functional properties. These degradation phenomena become extremely important in modern technologies operating with micro- and nanoscale films grown on foreign substrates. Well-known examples of thin film technologies include fabrication of semiconductor and piezoelectric heterostructures for electronic and optoelectronic application, hard films and coatings on metals as environmental and thermal barriers, and biological films and membranes for catalysis and sensing applications. Professor Wolfgang Pompe's research in the field of mechanics of thin film and composite materials forms a solid theoretical foundation that underpins our ability to bring the above technologies to fruition. It is difficult to overestimate the results of his work in this field, which has spanned over four decades (see, for example, Refs. [1-7]).

One physical source for mechanical stresses in thin films or surface layers is the variation of crystal lattice parameter in the film/layer under constraints caused by the underlying layer or the substrate. These lattice parameter variations can be caused by chemical composition changes, phase transformation, or an enhanced number of crystal lattice defects in the layer. The most practically relevant cases for stress manifestation in film/substrate systems include those originating from crystal lattice mismatch and a difference of thermal expansion coefficients between the film and the substrate, as well as grain coalescence in growing polycrystalline films, e.g. Ref. [8]. In the case of an abrupt change of the physical and chemical properties in the layer constrained by a very thick substrate, stresses develop only in the layer where they are usually uniform, e.g. Ref. [9]. In the general case, the magnitude of stresses may vary with depth beneath the free surface of layer. Obvious examples include functionally graded materials such as compositionally graded SiGe films [10] or graded materials for biomedical applications [4]. In this paper we consider another source of non-uniform stress profiles in surface layers, namely one related to the specific dislocation structures in growing a mismatching III-nitride layer. As has been established by recent experimental observations [11-13], initially compressed Al_xGa_{1-x}N layers can gradually diminish the magnitude of the stress when layer growth proceeds. We explain this phenomenon as a result of the intentional inclination of threading dislocations (i.e. dislocations extending through the layer) of edge character, which were originally oriented parallel to the c-axis of the wurtzite crystal structure of the $Al_xGa_{1-x}N$ layer [12, 14].

The magnitude of the stress field, the stressed volume, and the stored elastic energy usually increase as the layer growth proceeds. In such cases the total energy of the layer/substrate system can be diminished by the manifestation of relaxation processes accompanied by the change in defect structure, i.e. degradation of the system. Typically, misfit dislocations can form at the layer/substrate interface [9, 15] or cracks can develop in stressed layers or along the interface [9, 16].

For stressed mismatched III-nitride layers, both relaxation phenomena, i.e. misfit dislocation [17, 18] and crack [19, 20] formation, have been observed but have not yet received a complete theoretical description. Typically, III-nitride layers have a high density of threading dislocations [21], which in their turn can be involved in the onset of re-

Applied

Applied

laxation processes. The cracking of nitride layers often occurs in layers that are under nominal thermal mismatch compression at room temperature [22]. However, specially designed experiments [20, 22] confirm that cracks nucleate at the free surface of the growing films in the modes typical for fracture under tensile load. It was proposed that the stress state changed in the nitride layers with increasing thickness [20]. One possible mechanism could explain tensile stresses in the growing layers as a result of island coalescence providing that the layer grows in island mode [9]. However, as we will show below, cracking can be observed in nominally compressed at growth temperature $Al_xGa_{1-x}N$ films, which grew in a step-flow mode [11, 13] and therefore do not allow the realization of the coalescence mechanism. As was already mentioned, stress relaxation in nominally compressed layers can be achieved via threading dislocation inclination, which leads to a gradual reduction of the compressive stress [12, 14]. Subsequent layer growth can produce a gradient in tensile stress (i.e. increasing tensile stresses near the free surface), which at a certain thickness will initiate cracking through the layer.

The aim of the present article is to develop a fracture mechanics approach for the understanding of crack formation in surface layers with strain gradients and to compare the predictions of the continuum mechanics modeling with experimental observation of cracking in III-nitrides.

2. Motivation

Our modeling efforts are motivated by experiments on the observation of microcracks in Al_xGa_{1-x}N thin layers, which grow under nominal compression due to lattice mismatch with respect to an underlying buffer layer. We attribute the change of the stress state from compression to tension in the process of layer growth as the reason for the observed crack formation. The change in the stress state is due to the development of strain gradients caused by inclined threading dislocations with a misfit component.

2.1. Summary of experimental observation of relaxation and cracking in nominally compressed III-nitride layers

For the analysis of the crack formation under the condition of strain and stress gradients, Si-doped Al_{0.49}Ga_{0.51}N/ Al_{0.62}Ga_{0.38}N structures were grown on c-plane sapphire substrates by low pressure metalorganic chemical vapor deposition (MOCVD), as described previously in Refs. [11, 12]. The grown structures included a thin low temperature AlGaN nucleation layer followed by a $\sim 0.95 \,\mu m$ thick Al_{0.62}Ga_{0.38}N buffer layer grown at high temperature. Then, either a 130 nm thick or 750 nm thick Si-doped Al_{0.49}Ga_{0.51}N film was grown on top of the buffer layer at the same high temperature conditions. All structural studies showed that these layers grew in a step-flow mode. The structural properties of the Si-doped Al_{0.49}Ga_{0.51}N films were evaluated by atomic force microscopy (AFM), high-resolution X-ray diffraction (HRXRD), and transmission electron microscopy (TEM). The details on the growth and characterization techniques can be found in Refs. [11, 12, 23].

The stress/strain state in the Al_{0.49}Ga_{0.51}N layer was determined from the change of the crystal lattice parameters relative to those of the underlying Al_{0.62}Ga_{0.38}N layer by

the analysis of HRXRD reciprocal space maps. The degree of relaxation R (where R = 1 corresponds to fully relaxed and R = 0 corresponds to fully coherent layer) was R =1.01 for both the 130 and 750 nm thick layers. Note that a relaxation degree R > 1 indicates a change in stress state from compression to tension. We attribute R to the surface region of the film and accept this result for relaxation degree as an indication of no elastic strain at the layer surface. In the following we compare this with the magnitude of elastic strain calculated exactly at the surface. Combining the above results with the data for the layers of different thicknesses and with varying values of Si-doping [11, 12], one can deduce the linear dependence of the in-plane compressive stresses on the depth in the layer [12, 14] (the mathematical formula for this dependence is given in the next subsection). Similar results on the linear dependence of compressive stresses in undoped AlGaN layers were also reported in Ref. [13].

Optical microscopy studies of the 130 nm thick layer (Fig. 1a) show a good quality surface with no cracking

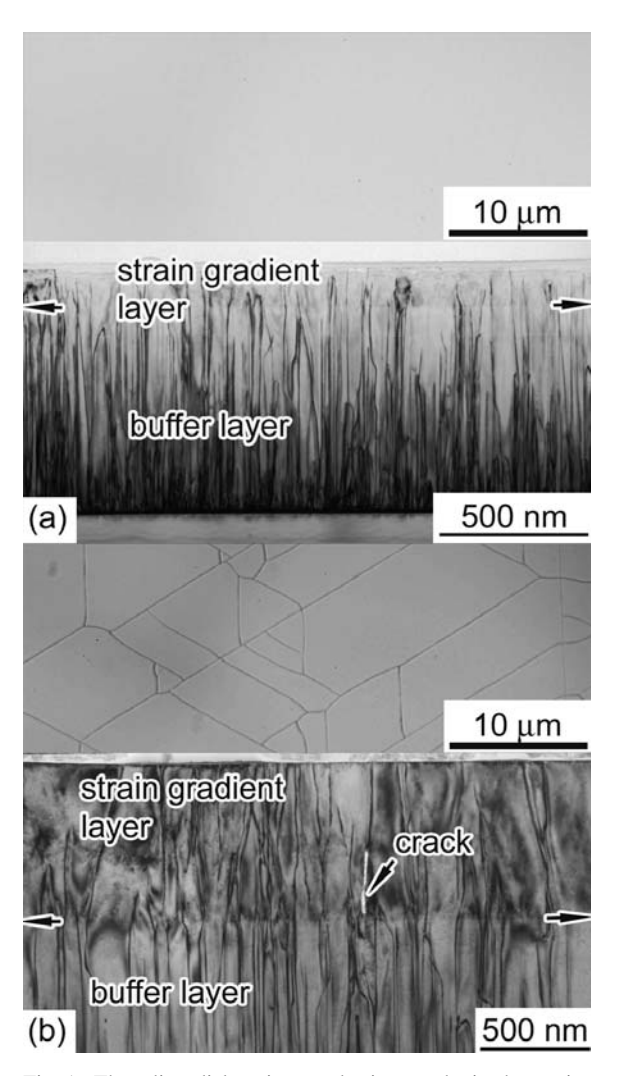


Fig. 1. Threading dislocations and microcracks in the strain gradient layer in Al_{0.49}Ga_{0.51}N/Al_{0.62}Ga_{0.38}N structure. The thickness of $Al_{0.49}Ga_{0.51}N$ layer is (a) ~ 130 nm; and (b) ~ 750 nm. Optical micrographs (top) and cross-section TEM images (bottom) of strain gradient layers recorded with g = 0002 two-beam imaging conditions are shown. The 130 nm thick layer demonstrates no cracking whereas the 750 nm thick layer shows cracks, which extended from mid-film thickness to the interface with the underlying Al_{0.62}Ga_{0.38}N buffer.

whereas optical microscopy of the 750 nm thick layer clearly indicates cracks with a $\sim 20 \, \mu m$ spacing (Fig. 1b). We believe that the similar relaxation degree for the 130 nm and 750 nm films is related to the cracking of the 750 nm thick film. Cracks in the film can relieve normal films stresses over lateral dimensions several times the film thickness. Cross-section TEM studies of the sample with the nominally 130 nm thick layer, Fig. 1a, show that the threading dislocations are inclined in the Al_{0.49}Ga_{0.51}N layer. The sample with the 750 nm thick layer, Fig. 1b, also demonstrates inclined threading dislocations in the Al_{0.49}Ga_{0.51}N layers but in addition shows cracks with openings from mid-depth in the Al_{0.49}Ga_{0.51}N layer to the bottom of the Al_{0.49}Ga_{0.51}N layer. The occluded crack indicated that the layer cracked during growth, providing stress relief, and then the crack was laterally overgrown.

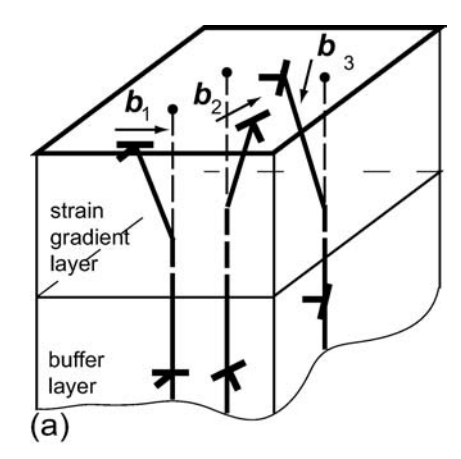
2.2. Role of dislocation inclination in generation of gradient elastic field in surface layers

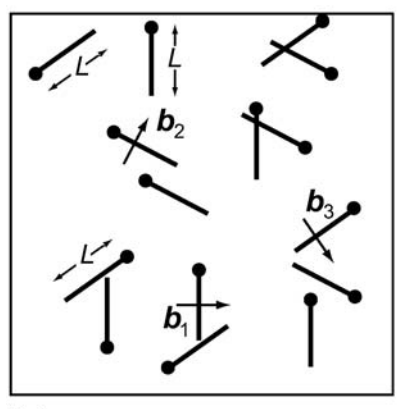
An approach for understanding the origin of the transition from compressive to tensile stresses in the surface layers of III-nitrides (grown in (0001) orientation of the surface) has been originally proposed in Ref. [11] and then developed in detail in Refs. [12, 14]. It has been clearly demonstrated that the stress variation in such gradient layers is caused by the inclined segments of threading dislocations of edge character with Burgers vectors of the type $\frac{1}{3}$ <11 $\frac{1}{2}$ 0> Such inclined dislocation segments can be seen in that part of the layer designated as the "strain gradient layer" in Fig. 1. In the buffer layer, these TDs have a [0001] line direction; however, in the compressed part of the surface layer, they become systematically inclined with respect to the [0001] growth direction by some angle α . The magnitude of the inclination angle a can be as large as 20° [11, 12, 13].

Figure 2 presents a schematic of edge threading dislocation inclination in III-nitride strain gradient layers. When viewed down the growth direction, the inclined threading dislocations have an average projected length L. The dislocation Burgers vectors are projected on the layer/substrate interface without any distortion. Therefore, in the far field, the projected dislocation segments are equivalent to the sections of misfit dislocations. Due to three-fold symmetry of the main crystallographic directions in the (0001) plane, the misfit dislocation segments can be combined into three families of straight line misfit dislocations along the projected directions of threading dislocation inclination. The total biaxial plastic relaxation at the top layer surface resulting from the triangular MD grid $\varepsilon_{\rm pl}^{\rm top}$ is given by [14]:

$$\varepsilon_{\rm pl}^{\rm top} = \frac{1}{2} b \rho_{\rm TD} L \tag{1}$$

where ho_{TD} is the threading dislocation density and L is the projected length of the threading dislocation segments, which is directly related to the layer thickness h and the inclination angle α by $L = h \tan \alpha$. For $\rho_{\text{TD}} = 3.0 \cdot 10^{10} \, \text{cm}^{-2}$, h = 200 nm, $\alpha = 17^{\circ}$, and b = 0.318 nm (corresponding to the observations in Refs. [11, 12]), Eq. (1) gives the plastic relaxation at the layer surface $\varepsilon_{\rm pl}^{\rm top} = 0.0029$ that is comparable with the initial misfit $\varepsilon_{\rm m} \approx 0.0032$ and the relaxation degree $R \approx 1$ of experimentally observed layers [11, 12].





(b)

Fig. 2. Schematic for inclined edge dislocations in a strain gradient layer. (a) three families of edge dislocations corresponding to three possible orientations of the Burgers vector in the (0001) plane of III-nitride layer; (b) plan-view presenting the average dislocation projected length \tilde{L} .

As a result of the plastic relaxation, the elastic strain dependence on position inside the strain gradient layer is giv-

$$\varepsilon_{xx} = \varepsilon_{yy} = \nabla \varepsilon_{nl} (h - z) - \varepsilon_{m}$$
 (2)

where h is the thickness of the layer with inclined threading dislocations, $\nabla \varepsilon_{\rm pl}$ is the strain gradient, which can be deduced from Eq. (1), $\varepsilon_{\rm m}$ is the magnitude of the initial compressive strain in the layer, which is also the magnitude of lattice mismatch, z is the distance taken from the layer surface (see the coordinate system in Fig. 3a). In practice, the gradient in strain relaxation $\nabla \varepsilon_{\rm pl}$ can be easily estimated from $\nabla \varepsilon_{\rm pl} = \varepsilon_{\rm m}/h_0$ where h_0 is the uncracked layer thickness of the complete strain relaxation (zero elastic strain) on its surface.

Non-zero stress components in the layer demonstrate similar linear dependence shown in Fig. 3b:

$$\sigma_{xx} = \sigma_{yy} = m(h - z) - \sigma_0, \ z < h \tag{3a}$$

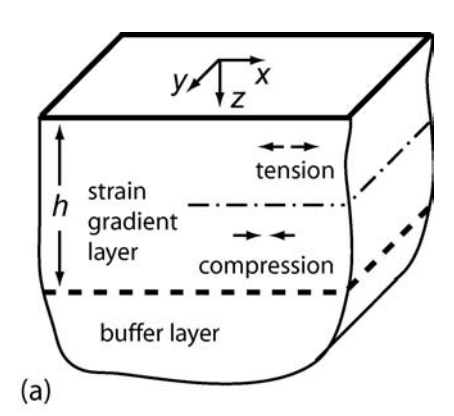
$$\sigma_{xx} = \sigma_{yy} = -\sigma_0, \ z \ge h \tag{3b}$$

where m is stress gradient defined as $m = \sigma_0/h_0$, and σ_0 is the initial magnitude of compressive stresses that is related to the equibiaxial mismatch ε_m :

$$\sigma_0 = M\varepsilon_{\rm m} \tag{4}$$

Applied





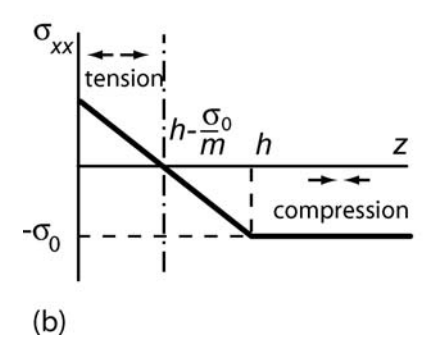


Fig. 3. Linear stress dependence in strain gradient layers. (a) schematic of the layer with a coordinate system xyz; (b) in-plane stress component σ_{xx} in dependence on the depth in the layer.

where the biaxial elastic modulus M can be given either for an isotropic material:

$$M_{\text{isotropic}} = \frac{E}{1 - v} \tag{5a}$$

where E is Young's modulus and ν is Poisson's ratio, or for wurtzite type semiconductors:

$$M_{\text{wurtzite}} = \frac{(C_{11} + C_{12}) C_{33} - 2C_{13}^2}{C_{33}}$$
 (5b)

where C_{kl} are the elastic stiffnesses. The value of σ_0 can be estimated for example for Al_{0.49}Ga_{0.51}N layer, which is matched to a $Al_{0.62}Ga_{0.38}N$ buffer. In this case $\varepsilon_m \approx$ 0.0032 [12] and the elastic constants C_{11} , C_{12} , C_{13} and C_{33} for the layer with ternary composition can be estimated by applying Vegard's Law to the known constants for GaN and AlN [24]. The result is $\sigma_0 \approx 1.47$ GPa. The stress gradient can be estimated by taking the experimentally determined value of $h_0 \approx 130 \text{ nm}$ that gives $m \approx$ 11.3 GPa μ m⁻¹ (or 10¹⁵ Pa m⁻¹). If this stress gradient is sustained during the layer growth, a high level of tensile stress can be generated in the surface part of the layer shown in Fig. 3.

3. Stress intensity factor for edge crack in strain gradient layer

Suppose that the level of the tensile stress on the surface is sufficient to induce cracking. We suppose an incipient mode I edge crack nucleates on the layer surface and propagates normally in the layer interior to depth a (see Fig. 4). We limit our consideration to the case where the crack front is relatively long along the y-axis and the crack plane re-

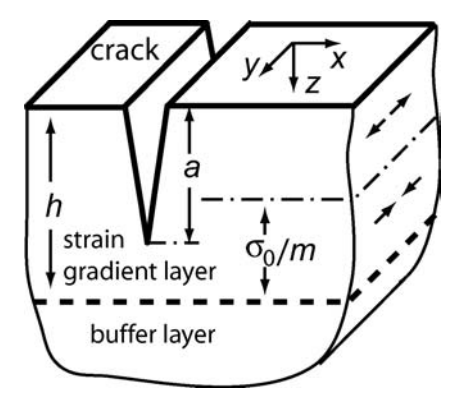


Fig. 4. Mode I edge crack in the strain gradient layer. h, a, σ_0 , m are parameters of the model, see explanation in the text.

mains perpendicular to the x-axis. We investigate the socalled "edging" crack propagation along the z-direction, which should be distinguished from a "channeling" crack propagation, where a pre-existing crack propagates along the y-direction in the layer [16]. The fact that there exists a tensile stress field acting perpendicular to the crack plane implies that some mode I stress intensity factor $K_{\rm I}$ will be induced at the crack tip that would be indicative of a driving force for crack extension, in accordance with linear elastic fracture mechanics theory. The stress intensity would depend on several variables, such as layer thickness h, the magnitude of the initial compressive stress σ_0 , the stress gradient m, and the crack length a. The stress intensity factor for a crack of prescribed length a can be determined through a superposition procedure described in [25], and is given by:

$$K_{\rm I} = \int_0^a \frac{2\sigma(z) F(z/a)}{\sqrt{\pi a} \sqrt{1 - \left(\frac{z}{a}\right)^2}} \, \mathrm{d}z \tag{6}$$

where $\sigma(z)$ is the stress along the plane in the *uncracked* solid where the crack is expected to occur. In our case $\sigma(z) = \sigma_{xx}(z)$, as given by Eq. (3).

Equation 6 originates from the weight function theory developed in fracture mechanics [26, 27]. The "kernel", or weight function, in Eq. (6) that is, every term in the integrand except $\sigma(z)$, is the stress intensity factor induced by a pair of collinear line loads of unit magnitude applied to the faces of an edge crack, at distance z from the free surface, that tend to open it. The weight function under consideration can be, for example, taken from [28]. It may be written in the following approximate form:

$$F(z/a) \approx 1.3 - 0.3 \left(\frac{z}{a}\right)^{5/4}$$
 (7)

After some algebraic manipulation (see, for example, [29]), Eq. (6) can be expressed in terms of a nonsingular integrand

$$K_{\rm I} = \sigma(a)\sqrt{\pi a} + \frac{2}{\sqrt{\pi a}} \int_{0}^{a} \frac{\left[\sigma(z)F(z/a) - \sigma(a)\right]}{\sqrt{1 - \left(\frac{z}{a}\right)^{2}}} \,\mathrm{d}z \tag{8}$$

For the stress gradient given by Eq. (3), the integration is performed analytically for both cases, i.e. when the crack is stopped in the strain gradient layer:

$$K_{\rm I} = \{ (mh - \sigma_0) \left[\pi + 0.6 f_1(1) \right] - ma \left[2 + 0.6 f_2(1) \right] \} \sqrt{\frac{a}{\pi}}, \ a < h$$
 (9a)

or when it is arrested in the compressed buffer:

$$\mathit{K}_{I} = \left\{ -\sigma_{0}[\pi + 0.6\mathit{f}_{1}(1)] + 0.6\mathit{mh}\left[\mathit{f}_{1}\left(\frac{h}{a}\right) - \frac{a}{h}\mathit{f}_{2}\left(\frac{h}{a}\right)\right] \right.$$

$$+2ma\left[\frac{h}{a}\sin^{-1}\frac{h}{a}+\sqrt{1-\left(\frac{h}{a}\right)^2}-1\right]\right\}\sqrt{\frac{a}{\pi}},\ a\geq h$$
(9b)

The functions $f_1(\xi)$ and $f_1(\xi)$ used in Eqs. (9a, b) are defined via Gauss hypergeometric function [30] ${}_2F_1(a,b;c,x)$:

$$f_1(\xi) \equiv \sin^{-1} \xi - \frac{4}{9} \xi^{9/4} {}_2 F_1\left(\frac{1}{2}, \frac{9}{8}; \frac{17}{8}, \xi^2\right)$$
 (10a)

$$f_2(\xi) \equiv 1 + \left(\frac{4}{9}\xi^{5/4} - 1\right)\sqrt{1 - \xi^2} - \frac{4}{9}\xi^{5/4} {}_2F_1\left(\frac{5}{8}, \frac{1}{2}, \frac{13}{8}, \xi^2\right) \tag{10b}$$

and have the numerical values $f_1(1) \approx 0.64$ and $f_2(1) \approx 0.25$.

We note that for a layer without a strain gradient m = 0 or for very small crack length a << h, we recover the expected, classical solution for an edge crack in a uniformly loaded semi-infinite space. Moreover, Eq. (9a) is consistent with a known solution for an edge crack in a half-space subject to a linearly varying traction [31].

4. Numerical results and discussion

Sample results for the $K_I(a)$ dependence via Eqs. (9a and b) are given in Fig. 5. For a given set of parameters, i.e. film thickness h, bulk value of compressive stress σ_0 , and stress gradient m, a general trend is that K_I initially increases with crack size. This means that the driving force for crack extension increases as the crack grows. Assuming the resistance to fracture remains constant, as is typical of brittle materials, this implies that unstable crack growth would occur if any fracture process were initiated. After reaching a maximum, the driving force decreases with increasing crack size. For large crack length the stress intensity factor becomes negative, that implies no driving force at all. Therefore, crack arrest will occur after some increment of instable crack growth.

We can define a critical thickness for crack formation in strain gradient layers by identifying the maximum $K_{\rm I}$ with the critical stress intensity factor for fracture, $K_{\rm Ic}$, and solving for h. Doing so yields the expression:

$$h_{\text{crit}} = \frac{\sigma_0}{m} + \frac{3\pi^{1/3} [2 + 0.6f_2(1)]^{1/3}}{[\pi + 0.6f_1(1)]} \left(\frac{K_{\text{Ic}}}{2m}\right)^{2/3}$$
(11a)

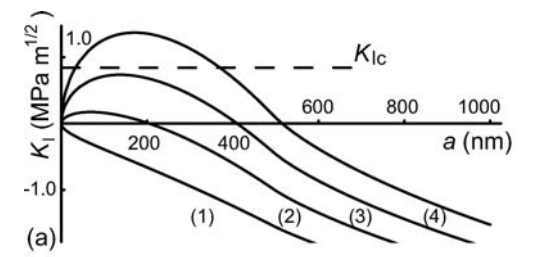
which (due to the fact that the first term is just h_0) can be rewritten in the following form

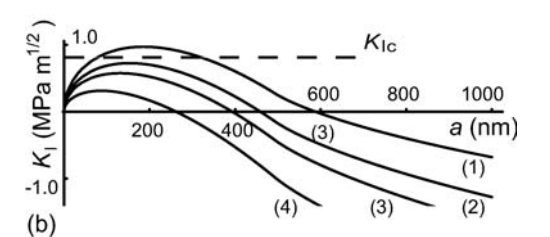
$$h_{\rm crit} = h_0 + \Delta h_{\rm crit} \tag{11b}$$

It is obvious that for strain gradient layer thickness less than $h_{\rm crit}$, the driving force for crack propagation remains insufficient to initiate fracture. Even if the condition $h > h_{\rm crit}$ is fulfilled, short surface cracks do not have enough driving force for their unstable growth, because their stress intensity factor is still lower than $K_{\rm Ic}$. This indicates a barrier for crack nucleation and assumes that additional stress concentrators such as surface flaws or defects can be important for the process of crack formation in strain gradient layers.

To estimate the typical value of $h_{\rm crit}$ one should substitute the experimentally determined value for stress gradient $m\approx 11.3$ GPa μm^{-1} [11, 12] together with an experimentally detrmined fracture toughness for GaN $K_{\rm Ic}\approx 0.8$ MPa $m^{1/2}$ [32] into Eq. (11). This gives $\Delta h_{\rm crit}\approx 173$ nm, i.e. $h_{\rm crit}\approx 303$ nm. The obtained result is in agreement with experimental observations (see Section 2 and Fig. 1), which show that nominally compressed Al $_{0.49}$ Ga $_{0.51}$ N layers with strain gradients have no cracks for thicknesses ~ 300 nm, but demonstrate cracks for thicknesses greater than ~ 400 nm.

The crack shown in the Fig. 1b resides deep within the layer with the strain gradient. This result is consistent with our predictions. The crack depth depends strongly on the value of the $K_{\rm Ic}$ and also on the layer thickness at which the crack was nucleated. From the experiment we do not know exactly at which thickness the crack appears and how the crack healing proceeds during the subsequent layer growth – this is a topic of ongoing investigation.





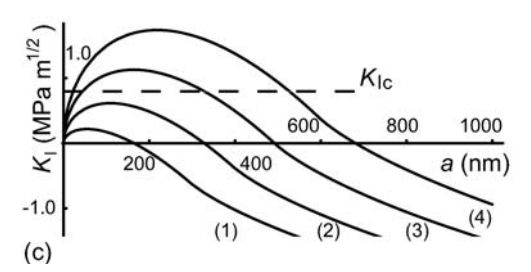


Fig. 5. Stress intensity factor K_1 for a crack in the strain gradient layer as function of the crack length a. (a) for layer thickness h=500 nm and initial compressive stress $\sigma_0=1.5$ GPa with varying stress gradient m=2.0 (1), 4.0 (2), 6.0 (3), 8.0 (4) \cdot 10¹⁵ Pa m⁻¹; (b) for layer thickness h=500 nm and stress gradient $m=5.0 \cdot 10^{15}$ Pa m⁻¹ with varying initial compressive stress level $\sigma_0=0.8$ (1), 1.1 (2), 1.4 (3), 1.7 GPa; (c) for initial stress $\sigma_0=1.4$ GPa and stress gradient $m=7.0 \cdot 10^{15}$ Pa m⁻¹ with varying layer thickness h=300 (1), 400 (2), 500 (3), 600 (4) nm. Experimental [32] value of fracture toughness for GaN $K_{\rm Ic}=0.8$ MPa m^{1/2} is given by a dashed line.

The framework presented here for crack formation in strain gradient layers with initial nominal compressive stresses can give predictions for crack formation for a number of experimentally relevant cases including not only IIInitride layers but also functionally graded layers of various origins. However, in the layers with strain gradients caused by dislocation inclination it can only operate when threading dislocations maintain their frozen-in inclined orientation. The reason why threading dislocations do not change their direction when the sign of the stress changes from compression to tension is unresolved. One speculation is that the growth with frozen-in threading dislocations is governed by local processes in the vicinity of dislocation intersection with a layer surface [12]. We also can comment on the results reported in the literature [20] indicating the presence of inclined dislocations, i. e. strain gradients, in initially compressed GaN layers undergoing a transition to tensile stress state with increasing the layer thickness.

5. Conclusions

The problem of crack fomation in surface layers with induced elastic strain and mechanical stress gradients has been addressed. We have demonstrated that the stress intensity factor $K_{\rm I}$ for a mode I edge crack is expressed in analytical form given by Eq. (9) as a function of crack length for the loading conditions typical for strain gradient layers. The critical layer thickness for crack formation in a gradient elastic field has been introduced and determined by comparing the driving force for crack extension in a gradient elastic field with the material fracture toughness K_{Ic} . It has been established that such stress/strain state profiles can be generated in functionally graded materials or due to specific stress relaxation mechanisms in lattice mismatched layers. This last mechanism works in nominally compressed AlGaN layers grown on lattice mismatched substrates with smaller lattice constants. It has been demonstrated that the magnitude of the stress gradient in the case of AlGaN layers is directly proportional to the tangent of the inclination angle of threading dislocations from the layer growth direction. The results of the modeling have been compared with experimental observations of crack onset in nominally compressed AlGaN layers undergoing transition to tensile stresses during growth. Good agreement between the model predictions and experimental data has been established both for the magnitude of strain gradient and for the critical thickness for crack formation.

The work was supported by the DARPA SUVOS program (H. Temkin, program manager) and by the Solid State Lighting and Display Center at UCSB. A. E. Romanov was supported by RFBR project 05-08-65503-a. The authors acknowledge the support of the National Science Foundation through the MRSEC Facilities.

References

- [1] R. Heinrich, W. Pompe: Phys. Stat. Sol. 40 (1970) 523.
- [2] W. Kreher, W. Pompe: J. Mech. Phys. Sol. 33 (1985) 419.
- [3] W. Pompe, X. Gong, Z. Suo, J.S. Speck: J. Appl. Phys. 74 (1993) 6012.
- [4] W. Pompe, H. Worch, M. Epple, W. Friess, M. Gelinsky, P. Greil, U. Hempel, D. Scharnweber, K. Schulte: Mater. Sci. Eng. A 362 (2003) 40.
- [5] N. Seriani, W. Pompe, L.C. Ciacchi: J. Phys. Chem. 110 (2006) 14860.

- [6] M. Schreiter, R. Gabl R.J. Lerchner, C. Hohlfeld, A. Delan, G. Wolf, A. Blueher, B. Katzschner, M. Mertig, W. Pompe: Sens. Actuators B 119 (2006) 255.
- [7] J. Hohage, W. Pompe: Thin Solid Films 515 (2006) 1767.
- [8] M.D. Thouless: Annu. Rev. Mater. Sci. 25 (1995) 69.
- [9] L.B. Freund, S. Suresh: Thin Film Materials: Stress, Defect Formation and Surface Evolution, Cambridge University Press (2003).
- [10] Y. Shiraki, A. Sakai: Surf. Sci. Rep. 59 (2005) 153.
- [11] P. Cantu, F. Wu, P. Waltereit, S. Keller, A.E. Romanov, U.K. Mishra, S.P. DenBaars, J.S. Speck: Appl. Phys. Lett. 83 (2003) 674
- [12] P. Cantu, F. Wu, P. Waltereit, S. Keller, A.E. Romanov, S.P. Den-Baars, J.S. Speck: J. Appl. Phys. 97 (2005) 103534.
- [13] D.M. Follstaedt, S.R. Lee, P.P. Provencio, A.A. Allerman, J.A. Floro, M.H. Crawford: Appl. Phys. Lett. 87 (2005) 121112.
- [14] A.E. Romanov, J.S. Speck: Appl. Phys. Lett. 83 (2003) 2569.
- [15] R. Beanland, D.J. Dunstan, P.J. Goodhew: Adv. Phys. 45 (1996) 87.
- [16] J.W. Hutchinson, Z. Suo: Adv. Appl. Mech. 29 (1992) 63.
- [17] S. Srinivasan, L. Geng, R. Liu, F.A. Ponce, Y. Narukawa, S. Tanaka: Appl. Phys. Lett. 83 (2003) 5187.
- [18] J.A. Floro, D.M. Follstaedt, P. Provencio, S.J. Hearne, S.R. Lee: J. Appl. Phys. 96 (2004) 96, 7087.
- [19] N. Itoh, J.C. Rhee, T. Kawabata, S. Koike: J. Appl. Phys. 58 (1985) 1828.
- [20] L.T. Romano, C.G. Van de Walle, J.W. Ager III, W. Gotz, R.S. Kern: J. Appl. Phys. 87 (2000) 7745.
- [21] X.H. Wu, P. Fini, E.J. Tarsa, B. Heying, S. Keller, U.K. Mishra, S.P. DenBaars, J.S. Speck: J. Cryst. Growth 189/190 (1998) 231.
- [22] E.V. Etzorn, D.R. Clarke: J. Appl. Phys. 89 (2001) 1025.
- [23] A.E. Romanov, G.E. Beltz, P. Cantu, F. Wu, S. Keller, S.P. Den-Baars, J.S. Speck: Appl. Phys. Lett. 89 (2006) 161922.
- [24] A.F. Wright: J. Appl. Phys. 82 (1997) 2833.
- [25] T.L. Anderson: Fracture Mechanics: Fundamentals and Applications, 2nd Edn., Ann Arbor, CRC Press (1995).
- [26] H.F. Bueckner: Z. Angew. Math. Mech. 50 (1970) 529.
- [27] J.R. Rice: Int. J. Solids Struct. 8 (1972) 751.
- [28] H. Tada, P.C. Paris, G.R. Irwin: The Stress Analysis of Cracks Handbook, 3rd Edn., ASME, New York (2000).
- [29] A.J. Monkowski, G.E. Beltz: Int. J. Solids Struct. 42 (2005) 581.
- [30] A.P. Prudnikov, Y.A. Brychkov, O.I. Marychev: Integrals and Series: Special Functions, Nauka, Moscow (1983).
- [31] Stress intensity factors handbook, Ed. Y. Murakami, Pergamon, New York (1987).
- [32] M.D. Drory, J.W. Ager, T. Suski, I. Grzegory, S. Porowsky: Appl. Phys. Lett. 69 (1996) 4044.

(Received March 12, 2007; accepted April 27, 2007)

Bibliography

DOI 10.3139/146.101524 Int. J. Mat. Res. (formerly Z. Metallkd.) 98 (2007) 8; page 723–728 © Carl Hanser Verlag GmbH & Co. KG ISSN 1862-5282

Correspondence address

Prof. Dr. Sci. Alexei E. Romanov Ioffe Physico-Technical Institute, Russian Academy of Sciences Polytechnicheskaya 26, Saint Petersburg, R-194021, Russia Tel.: +78122927304

Fax: +78122927304 Fax: +78122941017 E-mail: aer@mail.ioffe.ru

You will find the article and additional material by entering the document number MK101524 on our website at www.ijmr.de